# SERCaMP: a carboxy-terminal protein modification that enables monitoring of ER calcium homeostasis

Mark J. Henderson, Emily S. Wires, Kathleen A. Trychta, Christopher T. Richie, and Brandon K. Harvey
Intramural Research Program, National Institute on Drug Abuse, Baltimore, MD 21224

**ABSTRACT** **Endoplasmic reticulum (ER) calcium homeostasis is disrupted in diverse pathologies, including neurodegeneration, cardiovascular diseases, and diabetes. Temporally defining calcium dysregulation during disease progression, however, has been challenging. Here we describe secreted ER calcium-monitoring proteins (SERCaMPs), which allow for longitudinal monitoring of ER calcium homeostasis. We identified a carboxy-terminal modification that is sufficient to confer release of a protein specifically in response to ER calcium depletion. A *Gaussia* luciferase (GLuc)–based SERCaMP provides a simple and sensitive method to monitor ER calcium homeostasis in vitro or in vivo by analyzing culture medium or blood. GLuc-SERCaMPs revealed ER calcium depletion in rat primary neurons exposed to various ER stressors. In vivo, ER calcium disruption in rat liver was monitored over several days by repeated sampling of blood. Our results suggest that SERCaMPs will have broad applications for the long-term monitoring of ER calcium homeostasis and the development of therapeutic approaches to counteract ER calcium dysregulation.**

**Monitoring Editor**
Reid Gilmore
University of Massachusetts

Received: Jun 20, 2014
Revised: Jul 3, 2014
Accepted: Jul 8, 2014

## INTRODUCTION

Endoplasmic reticulum (ER) calcium is necessary for numerous intrinsic ER functions, including protein folding (Burdakov *et al.*, 2005), lipid metabolism (Fu *et al.*, 2011), and trafficking of proteins through the secretory pathway (Di Jeso *et al.*, 1998). In addition, the gradient created across the ER membrane is necessary for calcium-dependent signaling pathways, the regulation of vesicle trafficking (Micaroni, 2010), and ER–mitochondria cross-talk (Mattson *et al.*, 2000). Calcium in the ER lumen is maintained at concentrations 1000- to 10,000-fold greater than in the cytoplasm by the sarco/endoplasmic reticulum $Ca^{2+}$ ATPase (SERCA), a pump that transports $Ca^{2+}$ ions from the cytoplasm into the ER lumen. The majority of calcium efflux from the ER is mediated by the ryanodine receptor (RyR) and inositol triphosphate receptor (IP3R), calcium channels that are activated by various cellular signals (Lanner *et al.*, 2010; Taylor and Tovey, 2010). Depletion of the ER calcium store can reduce chaperone activity and thereby activate the unfolded protein response, a set of cellular adaptations that can have both helpful and harmful effects (Rutkowski and Kaufman, 2004). The importance of tight control over ER calcium is demonstrated by polymorphisms that alter function of SERCA (Brody's disease and Darier's disease; Odermatt *et al.*, 1996; Sakuntabhai *et al.*, 1999) and RyR (malignant hyperthermia) (Gillard *et al.*, 1992). Dysregulated ER calcium homeostasis is also implicated in cardiac disease, diabetes, cancer, and neurologic diseases, among others (Mekahli *et al.*, 2011). A common feature of these diverse pathologies is the depletion of ER calcium, and approaches to reverse this process have great therapeutic potential.

Delineating the causal relationship between ER calcium imbalance and disease progression is challenging due to limitations in available methodologies. The development and recent improvement of calcium-sensitive dyes and fluorescent proteins has led to

This article was published online ahead of print in MBoC in Press (http://www.molbiolcell.org/cgi/doi/10.1091/mbc.E14-06-1141) on July 16, 2014.

Address correspondence to: Brandon K. Harvey (BHarvey@intra.nida.nih.gov).

Abbreviations used: AAV, adeno-associated virus; CPA, cyclopiazonic acid; DMC, 2,5-dimethyl-celecoxib; DTT, dithiothreitol; ER, endoplasmic reticulum; GFP, green fluorescent protein; GLuc, *Gaussia* luciferase; IP3R, inositol triphosphate receptor; KDELR, Lys-Asp-Glu-Leu endoplasmic reticulum protein retention receptor; MANF, mesencephalic astrocyte-derived neurotrophic factor; PCN, primary cortical neuron; RyR, ryanodine receptor; SERCA, sarco/endoplasmic reticulum calcium ATPase; SERCaMP, secreted ER calcium-monitoring protein; Tg, thapsigargin; TPEN, tetrakis-2-pyridylmethyl-ethylenediamine.

significant advances in measuring ER calcium in vitro (Palmer *et al.*, 2004; Rehberg *et al.*, 2008; Tang *et al.*, 2011). These approaches, however, have limitations that prevent them from being used in extended studies, which are often required to model disease progression. For example, assessing ER calcium in whole tissue is limited to single–time point ex vivo analyses or surgery to visualize the tissue of interest (Hara *et al.*, 2004). Our goal was to develop an approach to longitudinally monitor ER calcium homeostasis in vitro and in vivo, thereby providing a platform to investigate the contribution of ER calcium imbalance to disease pathogenesis.

Our recent study demonstrated that the carboxy-terminal sequence of mesencephalic astrocyte-derived neurotrophic factor (MANF), alanine-serine-alanine-arginine-threonine-aspartic acid-leucine (ASARTDL), was required for its secretion in response to ER stress (Henderson *et al.*, 2013). Here we determined that the C-terminal ASARTDL sequence is sufficient to specifically confer ER calcium-depletion-dependent secretion when appended to unrelated secreted proteins. We developed and characterized a *Gaussia* luciferase-based secreted ER calcium-monitoring protein (SERCaMP), which can be used to monitor ER calcium homeostasis over time via sampling extracellular fluids both in vitro and in vivo. Overall the ability to create proteins that are released in response to ER calcium depletion has great potential for examining the relationship between ER calcium and pathogenesis, for use as a biomarker of disease states, and possibly for regulating the release of therapeutic proteins.

## RESULTS

### Analysis of reporters tagged with KDEL-like C-terminal sequences

Our previous studies revealed that the ASARTDL sequence of MANF was required for thapsigargin (Tg)-induced secretion (Henderson *et al.*, 2013). To further assess the properties of the ASARTDL sequence, we created SH-SY5Y neuroblastoma cell lines that stably express green fluorescent protein (GFP)–ASARTDL, GFP-ASAKDEL (KDEL = canonical ER retention signal), or untagged GFP (Figure 1A). The signal peptide of MANF was appended to the N-terminus of each construct to allow access to the secretory pathway. As expected, we observed intracellular retention of the ASARTDL and ASAKDEL variants and increased secretion of the untagged variant (Figure 1, B–D). We next examined secretory responsiveness to Tg and observed a dose-dependent increase in secreted GFP-ASARTDL (Figure 1E).

Owing to limitations imposed when using GFP as a reporter—primarily low signal-to-noise ratio when sampling from culture media—we created a set of *Gaussia* luciferase (GLuc)–based reporters. In addition to the aforementioned carboxy-terminal sequences, we constructed two additional variants: RTDL (lacking ASA) and ASAKTEL (KTEL = C-terminus of cerebral dopamine neurotrophic factor, or CDNF, a homologue of MANF; Lindholm *et al.*, 2007; Figure 1F). Successful targeting of GLuc-ASARTDL to the ER was demonstrated by immunofluorescence analysis (Figure 1G). To confirm the Tg-inducible secretion, we tested four independently derived stable cell lines expressing GLuc-ASARTDL and observed a dose-dependent increase in secretion for all lines tested (Supplemental Figure S1A). Using recombinant GLuc protein, we observed a linear relationship between luminescence and GLuc concentration in culture medium between 1 pg/ml and 1 µg/ml (Supplemental Figure S1B). The sensitivity of the GLuc assay enabled detection of Tg-induced release of GLuc-ASARTDL from <20 cells (Figure 1H and Supplemental Figure S1C). We next compared secretion of the GLuc variants with unique C-terminal tails. Untagged GLuc exhibited the highest basal secretion (Figure 1I), and GLuc-ASARTDL had the greatest secretory response to Tg (Figure 1J). The untagged GLuc showed a minimal response to Tg and serves as a control for nonspecific effects on global secretion in subsequent experiments. Although the majority of our experiments use cells stably expressing GLuc-ASARTDL, we also observed Tg-inducible secretion in a transient transfection model (Supplemental Figure S1, D and E). In addition, we observed similar results when the endogenous signal peptide of GLuc was used in place of the MANF signal peptide (Supplemental Figure S1F).

### GLuc-ASARTDL secretion does not occur in response to all forms of ER stress

A major effect of Tg treatment is the induction of an ER stress response (ERSR), and we speculated that activation of this pathway might contribute to release of ASARTDL-tagged proteins. We compared the timing of GLuc-ASARTDL release to up-regulation of the ER chaperone BiP (GRP78), a classic marker of ERSR activation (Lee, 2005). Secreted GLuc was stable, once released into culture medium (Supplemental Figure S1G), and therefore accumulates after release. To assess the timing of GLuc-ASARTDL release relative to Tg, a small volume of medium (5 µl) was collected and measured at multiple time points (repeatedly from the same well) and compared with the time-matched vehicle control. The levels of secreted GLuc-ASARTDL increased before the increase in intracellular BiP protein (Figure 2, A and B). The relatively rapid accumulation of GLuc-ASARTDL in the medium suggested that the secretion response was not dependent on ERSR transcriptional events. We confirmed that Tg-induced GLuc-ASARTDL secretion did not require new protein synthesis, using a 1-h pretreatment with cycloheximide (Supplemental Figure S2A); however, active trafficking through the classic secretory pathway was required based on inhibition with brefeldin A (Supplemental Figure S2C). Neither BFA nor cycloheximide pretreatment altered cell viability, as assessed by MTS assay (Supplemental Figure S2, B and D). These results support a model in which ASARTDL-tagged proteins are maintained in the ER and traverse the secretory pathway in response to a cellular stress signal.

To further examine the relationship between secretion and ER stress, we tested additional stress-inducing compounds. A glycosylation inhibitor, tunicamycin, and reducing agent, dithiothreitol (DTT), both failed to increase the level of secreted GLuc-ASARTDL (Figure 2C) despite their ability to activate ERSR as shown by BiP up-regulation (Figure 2D) and decreased cell viability (Supplemental Figure S2H). To rule out the possibility that these compounds were preventing proper folding and maturation of GLuc, which would preclude ER stress–induced release, cells exposed to tunicamycin or DTT were subsequently treated with Tg. The GLuc-ASARTDL protein was in fact mature and still "secretable" in the presence of tunicamycin and DTT, further supporting the interpretation that release of ASARTDL-tagged proteins is not a general response to ER stress (Figure 2, E and F). Of note, secretion of ASARTDL-tagged GFP was also unresponsive to tunicamycin or DTT treatment (Supplemental Figure S2, E and F). In addition, release does not appear to be a general consequence of cell death, as there was no correlation between cell viability and extracellular GLuc-ASARTDL when a panel of stress-inducing molecules was assessed (Supplemental Figure S2, G and H).

### GLuc-ASARTDL is secreted in response ER calcium imbalance

Thapsigargin disrupts ER calcium homeostasis by irreversibly inhibiting the ER calcium ATPase, SERCA (Davidson and Varhol, 1995). To

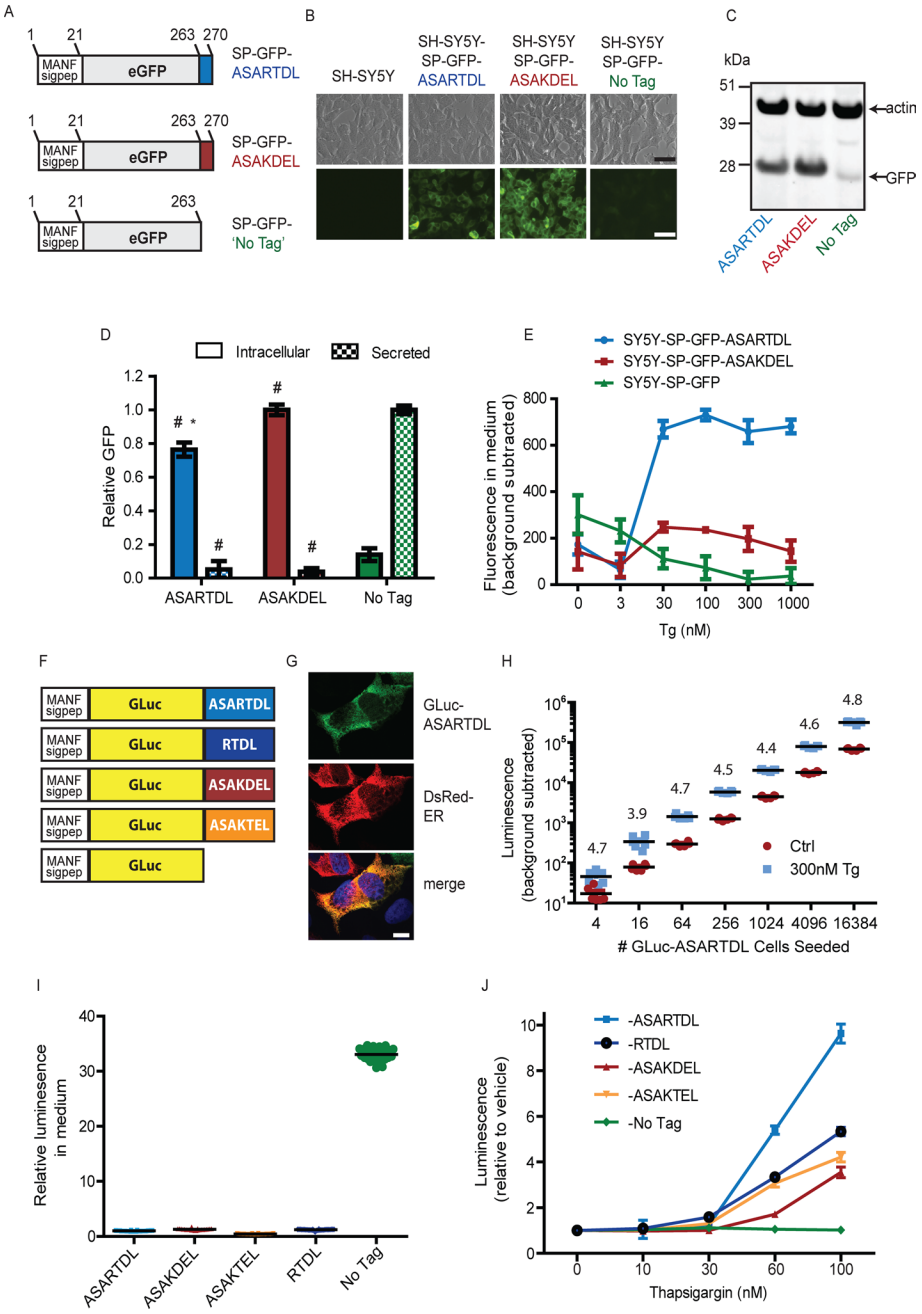


FIGURE 1: Creating a SERCaMP using a carboxy-terminal ASARTDL tag. (A) GFP-fusion proteins were constructed to study the secretory properties of C-terminal ASARTDL and ASAKDEL sequences. The signal peptide of MANF was appended upstream of GFP to target the proteins to the secretory pathway. (B) GFP-ASARTDL and GFP-ASAKDEL show increased intracellular fluorescence compared with untagged GFP by epifluorescence microscopy. Scale bar, 100 μm. (C) Intracellular levels of the GFP variants were examined by immunoblot. (D) Comparison of intracellular and secreted GFP. Intracellular levels were analyzed by densitometry of GFP immunoblots and normalized to actin (mean ± SD, $n = 3$, one-way analysis of variance [ANOVA], $p < 0.001$; $^{*}p < 0.001$, Newman–Keuls multiple comparison test vs. ASAKDEL; $^{\#}p < 0.001$, Newman–Keuls multiple comparison test vs. No Tag). Secreted levels were examined by measuring fluorescence of medium collected from cells (mean ± SD, $n = 4$, one-way ANOVA, $p < 0.001$; $^{\#}p < 0.001$ by Newman–Keuls multiple comparison test vs. No Tag). (E) Secretion of GFP-ASARTDL is more responsive to thapsigargin than GFP-ASAKDEL (mean ± SD, $n = 4$). (F) Schematic of *Gaussia* luciferase (GLuc) fusion proteins. This first 18 aa of GLuc (MGVKVLFALICIAVAEAK, signal sequence) were replaced with the signal sequence of MANF (aa 1–23, MWATQGLAVALALSVLPGSRALR). The final amino acids of MANF (ASARTDL), or additional similar sequences, were appended to the C-terminus. (G) GLuc-ASARTDL localizes to the ER of SH-SY5Y cells. SH-SY5Y-GLuc-ASARTDL stable cells were transiently transfected with a DsRed-ER plasmid, immunostained with anti-GLuc, and examined by confocal microscopy (blue, 4′,6-diamidino-2-phenylindole [DAPI]). Scale bar, 10 μm. (H) The minimum number of GLuc-ASARTDL cells required for the secretion assay was assessed. SH-SY5Y-GLuc-ASARTDL cells were plated at the indicated densities (supplemented with parental SH-SY5Y to 50,000 cells/well, 96-well plate). After overnight incubation, cells were treated for 2 h with 300 nM Tg (or vehicle), and luciferase was measured in the medium (mean, $n = 6$). Thapsigargin-induced secretion (relative to vehicle) is indicated for each density. (I) Basal secretion of the GLuc variants was assessed 24 h after plating cells at equal density ($n = 30$ wells, normalized to ASARTDL variant). (J) SH-SY5Y cells stably expressing the carboxy-terminal GLuc variants were treated with Tg for 4 h, and medium was assayed for luminescence (mean ± SD, $n = 6$).

confirm the effect of SERCA inhibition on GLuc-ASARTDL release, we tested the reversible inhibitor cyclopiazonic acid (CPA; Seidler *et al.*, 1989), which dose dependently increased secretion of GLuc-ASARTDL (Figure 3A). Washout experiments revealed that a minimum of 20 min of CPA treatment triggered subsequent release of GLuc-ASARTDL over the next 2 h (Figure 3B). Hence, we hypothesized that release of ASARTDL proteins was due to alterations in ER calcium levels. Treatment of cells with A23187, a calcium ionophore that allows calcium ions to freely cross lipid bilayers, caused a dose-dependent release of GLuc-ASARTDL (Supplemental Figure S3A) but had a minimal effect on untagged GLuc (Figure 3C). SERCA inhibitors and A23187 deplete calcium in ER but also increase calcium in cytoplasm. To separate the contribution of cytoplasmic versus ER calcium on the release of ASARTDL proteins, we used the low-affinity calcium chelator tetrakis-2-pyridylmethyl-ethylenediamine (TPEN). This approach allowed for $Ca^{2+}$ depletion in high-concentration organellar compartments without a corresponding increase in cytoplasmic levels (Hofer *et al.*, 1998). We observed a dose-dependent increase in GLuc-ASARTDL release after 2 h of TPEN treatment (Supplemental Figure S3B). TPEN-induced release was not observed for untagged GLuc, which decreased after treatment (Figure 3D). These results support secretion of ASARTDL-tagged proteins in response to ER calcium depletion.

We predicted that inhibiting calcium efflux from the ER would reduce release of GLuc-ASARTDL. To delay ER calcium depletion in the presence of Tg, we treated cells

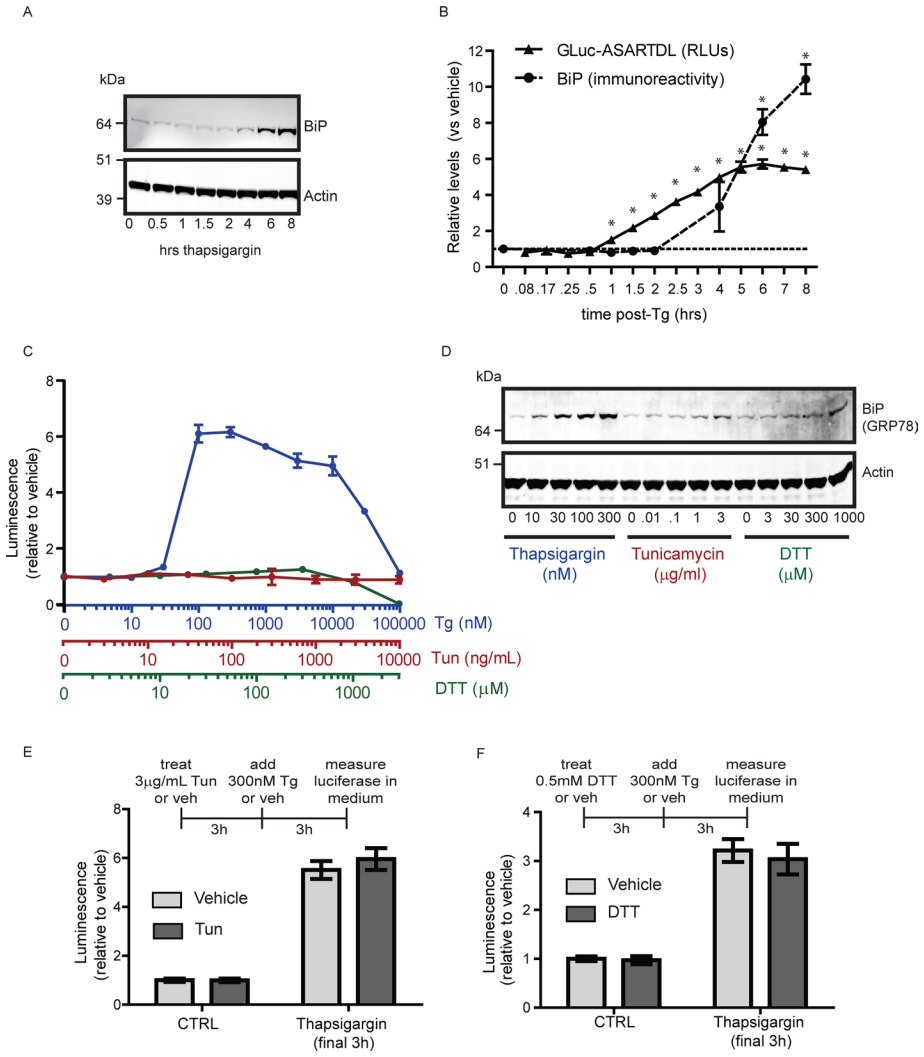


FIGURE 2: GLuc-ASARTDL release precedes BiP up-regulation and does not occur in response to all forms of ER stress. (A) Temporal analysis of BiP up-regulation in SH-SY5Y cells treated with 300 nM thapsigargin. Cells were lysed at the indicated time points after treatment and lysates examined by immunoblot for BiP. (B) Release of GLuc-ASARTDL precedes BiP up-regulation. Luciferase activity was compared with BiP protein levels in SH-SY5Y cells treated with 300 nM Tg. BiP protein levels are relative to expression at $t = 0$ (mean ± SD, $n = 3$, one-way ANOVA, $p < 0.001$; $^*p < 0.05$ by Dunnett's multiple comparison test). Secreted luciferase values were normalized to the vehicle control at each time point to examine the Tg-induced release (mean ± SD, $n = 6$, one-way ANOVA, $p < 0.001$), $^*p < 0.05$ by Dunnett's multiple comparison test). (C) SH-SY5Y cells stably expressing GLuc-ASARTDL were incubated with increasing concentrations of thapsigargin (blue), tunicamycin (red), or DTT (green) for 6 h. Secreted luciferase was measured (mean ± SD, $n = 3$). (D) DTT and tunicamycin treatment elevate BiP expression but do not alter secretion of GLuc-ASARTDL. Lysates were collected from cells (treated as described in C) and immunoblotted for BiP and actin. (E) GLuc-ASARTDL in tunicamycin-treated cells remains "secretable." Cells were treated with 3 μg/ml tunicamycin for 3 h, followed by 300 nM thapsigargin for 3 h. Luciferase activity was measured in the medium (mean ± SD, $n = 12$). (F) GLuc-ASARTDL in DTT-treated cells remains "secretable." Cells were treated with 500 μM DTT for 3 h, followed by 300 nM thapsigargin for an additional 3 h. Luciferase activity was measured in the medium (mean ± SD, $n = 12$).

with dantrolene and xestospongin C to inhibit ryanodine and IP3 receptors, respectively. Dantrolene dose dependently inhibited Tg-induced release (Figure 3E) but had no effect on untagged GLuc secretion (Figure 3F). Inhibition of IP3R with xestospongin C showed a minimal effect on secretion (Supplemental Figure S3C) and no effect on cell viability (Supplemental Figure 3D). To examine the possibility that RyR activity may compensate during IP3R inhibition, we tested for synergism of the two compounds. We observed no change from the individual treatments, suggesting that the release mechanism is primarily associated with RyR-regulated $Ca^{2+}$ pools in SH-SY5Y cells (Supplemental Figure S3E). Neither dantrolene nor xestospongin C nor the combination treatment had an effect on cell viability as assessed by ATP assay (Supplemental Figure S3F). On the basis of these results implicating RyR activity, we hypothesized that caffeine, a RyR agonist at high concentrations, would induce ER $Ca^{2+}$ depletion and augment secretion of GLuc-ASARTDL. We observed a dose-dependent release in response to caffeine (Figure 3G and Supplemental Figure S3G), whereas untagged GLuc release was inhibited (Figure 3G). We tested an additional agonist of the RyR, 4-chloro-*m*-cresol (Herrmann-Frank *et al.*, 1996), which increased release and augmented Tg-induced GLuc-ASARTDL release (Figure 3H).

## GLuc-ASARTDL release is regulated by the KDEL receptor

To gain insight into the mechanism of release in response to calcium depletion, we examined the contribution of the Lys-Asp-Glu-Leu endoplasmic reticulum protein retention receptor (KDELR). The RTDL sequence is structurally similar to the canonical KDEL sequence, which interacts with KDELRs as part of the Golgi-to-ER protein retrieval system (Raykhel *et al.*, 2007). Our previous work revealed that secretion of the neurotrophic factor MANF (ASARTDL protein) is modulated by KDELRs (Henderson *et al.*, 2013). To determine whether GLuc-ASARTDL secretion is also affected by KDELRs, we overexpressed KDELR in the stable reporter cell lines. Increasing the multiplicity of infection (MOI) of lentivirus encoding human KDELR decreased GLuc-ASARTDL secretion after Tg treatment, whereas virus containing noncoding vector had minimal effect (Figure 4, A and B). Furthermore, KDELR had no effect on untagged GLuc, indicating the ASARTDL is required for the KDELR effect on secretion (Figure 4C). To determine whether the ASARTDL directly interacts with the KDELR, we developed an enzyme-linked immunosorbent assay (ELISA) approach in which KDELR-myc-FLAG was captured in microwells using FLAG or myc antibodies (Supplemental Figure S4, A and B). When cell culture medium samples containing equivalent amounts of the GLuc-protein were incubated with the KDELR-coated plates, we observed increased retention of the ASAKDEL and ASARTDL variants compared with the untagged control, suggesting that there is a physical interaction between these sequences and the KDELR (Figure 4D). Overall these results demonstrate that the

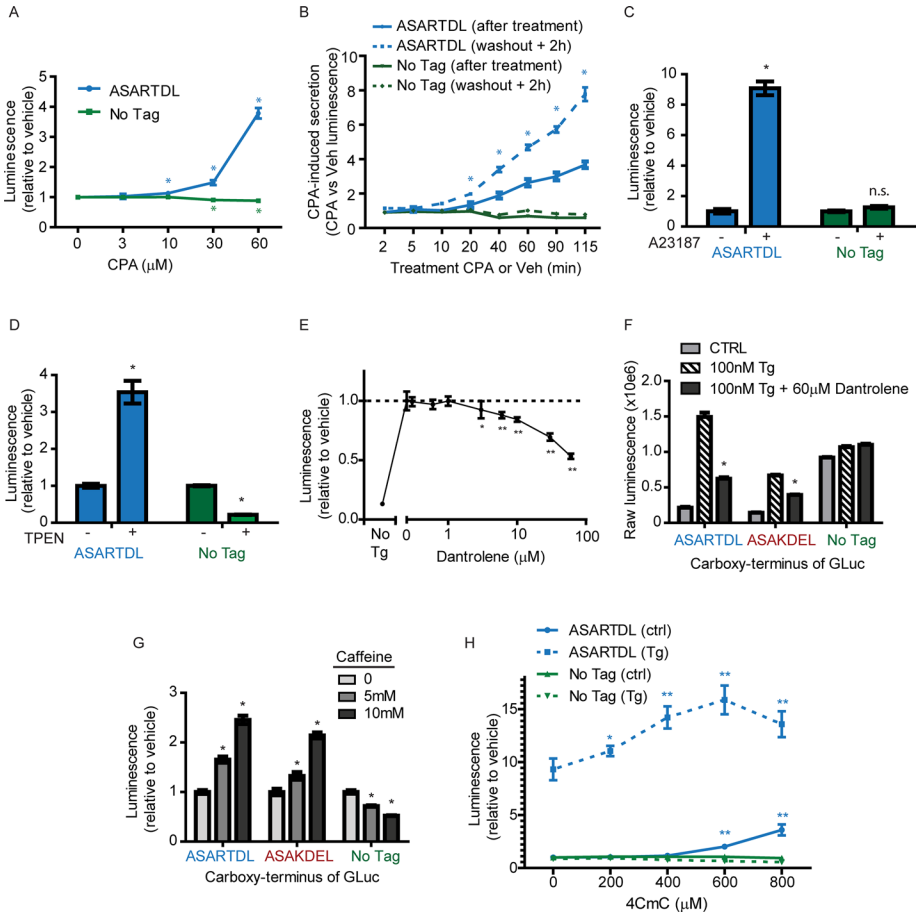


FIGURE 3: GLuc-ASARTDL secretion is triggered by ER calcium depletion. (A) SH-SY5Y stable cell lines were treated with the reversible SERCA inhibitor cyclopiazonic acid (CPA). After 6 h, luciferase was measured in the medium (mean ± SD, $n = 12$, one-way ANOVA, $p < 0.001$ for each variant; *$p < 0.001$ by Dunnett's multiple comparison test vs. vehicle control). (B) Stable cells were treated with 50 μM CPA for varying durations, followed by washout with six 50% medium exchanges. Luminescence values represent the CPA-induced response, as CPA-treated samples were normalized to the time-matched vehicle-treated wells. CPA-induced release was assessed immediately after treatment (solid lines) and 2 h after washout (dashed lines; mean ± SEM, $n = 12$, two-way ANOVA, $p < 0.001$; *$p < 0.001$ by Bonferroni multiple comparison test pretreatment vs. 2 h posttreatment). (C) The calcium ionophore A23187 increases secretion of GLuc-ASARTDL but has no effect on untagged GLuc. Cells were treated with 5 μM A23817, and luciferase activity was measured in the medium after 6 h (mean ± SD, $n = 8$, two-way ANOVA, $p < 0.001$ for treatment and cell line; *$p < 0.001$ by Bonferroni multiple comparisons). (D) The low-affinity calcium chelator TPEN induces secretion of GLuc-ASARTDL. Stable cells were treated with 1 mM TPEN as described in *Materials and Methods*, and luciferase activity was measured in the medium after 5 h (mean ± SEM, $n = 10$, two-way ANOVA, $p < 0.001$ for treatment and cell line; *$p < 0.01$ by Bonferroni multiple comparisons). (E) SH-SY5Y-GLuc-ASARTDL cells were pretreated with dantrolene for 30 min before addition of 300 nM thapsigargin. Luciferase activity was measured in the medium after 4 h (mean ± SD, $n = 6$, one-way ANOVA, $p < 0.001$; *$p < 0.05$; **$p < 0.001$ by Dunnett's multiple comparison test vs. vehicle control). (F) Stable SH-SY5Y cells were pretreated with 60 μM dantrolene for 30 min and treated with 300 nM thapsigargin for 6 h. Luciferase activity was measured in the medium (mean ± SD, $n = 8$, two-way ANOVA, $p < 0.001$ for treatment and cell line; *$p < 0.001$ by Bonferroni multiple comparisons Tg vs. Tg plus dantrolene). (G) Luciferase activity was measured in medium collected from stable cell lines 72 h after adding 1, 5, or 10 mM caffeine (mean ± SD, $n = 6$, two-way ANOVA, $p < 0.001$ for treatment and cell line; *$p < 0.001$ by Bonferroni multiple comparisons). (H) Stable cells were pretreated with 4-chloro-*m*-cresol (4CmC) or vehicle control for 30 min. Then 100 nM Tg or vehicle control was added, and GLuc was measured in the medium after 24 h (mean ± SD, $n = 6$, one-way ANOVA, $p < 0.001$; *$p < 0.05$, **$p < 0.001$ by Dunnett's multiple comparison test vs. vehicle control).

calcium-dependent secretion of ASARTDL can be modulated by KDELRs, potentially via changes to the direct interactions between the proteins.

## SERCaMP can be used in vitro to examine ER $Ca^{2+}$ dysregulation in primary neurons

The characteristics of GLuc-ASARTDL release suggest that it could be used as a reporter of ER calcium homeostasis in vitro and in vivo. To test the feasibility of this strategy in vitro, we developed a rat primary cortical neuron (PCN) model using adeno-associated virus (AAV) vectors (Figure 5A). We confirmed Tg-induced release from PCNs transduced with AAV-GLuc-ASARTDL, with elevated secretion observed as early as 2 h after treatment (Figure 5B). Release from PCNs was augmented by caffeine treatment (Supplemental Figure S5A) and inhibited by dantrolene (Supplemental Figure S5C), consistent with responsiveness to ER calcium depletion. In addition, overexpressing KDELR protein inhibited the Tg-induced release (Supplemental Figure S5D).

We next examined hyperthermia and glutamate toxicity, two physiologically relevant models of ER stress. Hyperthermia is a known activator of heat shock and ER stress response pathways (Xu *et al.*, 2011). Glutamate activates IP3Rs through metabotropic glutamate receptors, with excessive signaling causing ER stress–associated neurotoxicity (Sokka *et al.*, 2007). The effects of hyperthermia and glutamate toxicity on ER calcium, however, are not completely defined. We observed an increase in secretion of GLuc-ASARTDL from PCNs for each model, indicating that ER calcium depletion is caused by these insults (Figure 5, C–E). Hyperthermia showed a similar effect in the SH-SY5Y-GLuc-ASARTDL stable cell line (Supplemental Figure S6, A and B).

We also examined members of the cyclooxygenase-2 (COX-2) inhibitor (coxib) class of compounds, as recent evidence reveals that a subset of these drugs have off-target inhibitory effects on SERCA (Figure 5F, schematic; Johnson *et al.*, 2002; Pyrko *et al.*, 2007). As predicted, celecoxib and its noncoxib analogue 2,5-dimethyl-celecoxib (DMC) both increased secretion of GLuc-ASARTDL but had no effect on untagged GLuc (Figure 5, G and H). Valdecoxib, a coxib that has no reported activity on SERCA, did not alter the secretion of either variant (Figure 5, G and H). Of importance, dantrolene was able to diminish the effect of both DMC and celecoxib, implying that ER calcium depletion is a result of drug treatment (Figure 5I).

## Liver SERCaMP is released into the blood after SERCA inhibition

To verify that a SERCaMP could be used in vivo, we developed a model to monitor SERCaMP secretion from rat liver. A recent report demonstrated that direct injection of AAV into rat liver resulted in

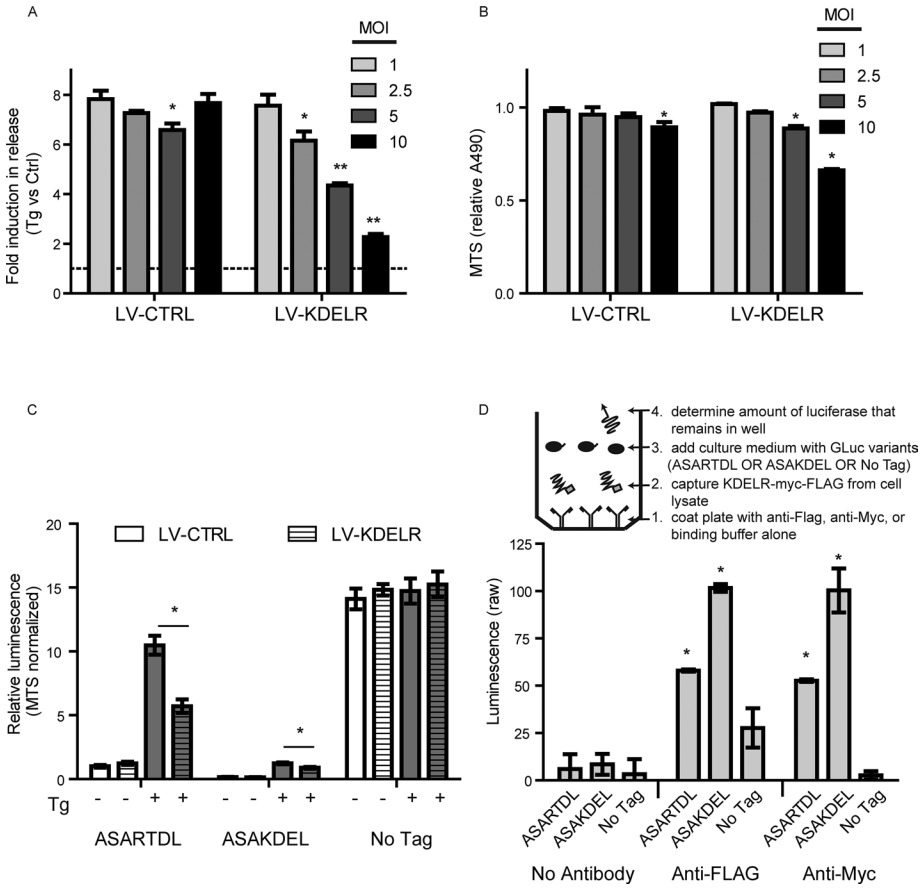


FIGURE 4: Secretion of GLuc-ASARTDL is modulated by KDELR expression. (A) SH-SY5Y-GLuc-ASARTDL cells were transduced with increasing MOIs of lentivirus encoding human KDELR2. At 48 h after transduction, medium was replaced; cells were incubated overnight and treated for 3 h with 100 nM Tg. Luciferase activity was measured in the medium (mean ± SD, $n = 3$, two-way ANOVA, $p < 0.001$ for virus and MOI; *$p < 0.05$, **$p < 0.001$ by Bonferroni multiple comparisons). (B) Cell viability at the time of luciferase assay was assessed by MTS assay (mean ± SD, $n = 3$, two-way ANOVA, $p < 0.001$ for virus and MOI; *$p < 0.05$ by Bonferroni multiple comparisons). (C) The effect of KDELR2 overexpression was examined in SH-SY5Y cells stably expressing GLuc-ASARTDL, GLuc-ASAKDEL, or untagged GLuc. Cells were transduced at a MOI of 5, incubated for 48 h, and incubated overnight after a medium exchange. Cells were then treated with 100 nM thapsigargin or vehicle control for 3 h, and luciferase activity was measured in the medium. Luminescence values were normalized using a MTS assay to account for changes in cell viability caused by KDELR2 overexpression (mean ± SD, $n = 4$, *$p < 0.01$, multiple $t$ tests with Holm-Sidak correction). (D) Inset, design of capture ELISA approach. The amount of GLuc variants that remained associated with KDELR1-coated wells was determined (mean ± SEM, $n = 3$ wells,*$p < 0.01$ vs. corresponding signal in the no-antibody control wells by Tukey's multiple comparison test).

detectable levels of a cytoplasmic luciferase protein (Sobrevals *et al.*, 2012). We used a similar approach, with rats receiving intrahepatic injections of AAV-GLuc-ASARTDL (Figure 6A). SERCaMP expression in the liver was confirmed by immunostaining (Figure 6B and Supplemental Figure S7A), and enzymatic activity was detectable in the blood, with a linear relationship between GLuc concentration and activity (Supplemental Figure S7B). By intravenous injection of GLuc-ASARTDL protein into naive rats, we calculated the half-life to be <5 min in circulation (Figure 6C). This suggests that changes in plasma GLuc-ASARTDL secreted from the liver represent an increase in the rate of secretion proximal to the time of sampling and not a protracted accumulation over days.

A single intraperitoneal (i.p.) injection of thapsigargin at 1 mg/kg (day 12 post-AAV) resulted in an increase in GLuc-ASARTDL plasma levels, which persisted for 3 d (Figure 6D). The response to thapsigargin was similar over a 100-fold range of AAV titers delivered intrahepatically ($7.6 \times 10^7$ to $7.6 \times 10^9$ viral genomes [vg]), suggesting that a range of SERCaMP transgene expression is possible for in vivo experiments (Figure 6D). At a viral titer of $7.5 \times 10^{10}$ vg, however, we observed a rapid and complete loss of enzymatic activity between days 7 and 17 (without Tg exposure), possibly due to an immunologic response to the transgene (Supplemental Figure S7C).

We next compared the Tg-induced response of GLuc-ASARTDL to the untagged control. The effect of gas anesthesia on GLuc secretion was assessed by subjecting the animals to three rounds of blood collection before the Tg challenge, which resulted in no appreciable change in GLuc in plasma (Figure 6E, –24 through 0 h). A single 1 mg/kg thapsigargin exposure resulted in a small but significant increase in GLuc–No Tag at the 50-h time point but less induction relative to the ASARTDL variant (Figure 6E, dark gray shaded box). GLuc levels returned to baseline between 3 and 6 d post-Tg, consistent with elevated secretion in response to Tg exposure. Together these data support the further use and development of SERCaMPs as genetically encoded biosensors for monitoring ER calcium dysfunction.

## DISCUSSION

Our results demonstrate that the carboxy-terminal SERCaMP modification (ASARTDL) can be used to create a reporter protein that enables monitoring of ER calcium depletion caused by pharmacological and pathological conditions (Figure 7). With the robust brightness of GLuc, we were able to detect calcium depletion in as few as 16 cells in culture (Figure 1H). This sensitivity provided an optimal platform to assess the utility of the reporter in vivo, where small volumes of blood (or other body fluids) can be sampled. Previous work indicated that GLuc can be measured in blood and urine from rats (Badr *et al.*, 2007), and our in vivo studies reveal that GLuc-ASARTDL is detectable in blood when expressed in the liver. The observed increase in GLuc-ASARTDL in circulation after thapsigargin exposure, followed by a return to preexposure levels, indicates the potential of SERCaMPs for longitudinally monitoring ER calcium homeostasis in living organisms.

The sum of our data supports a model in which a carboxy-terminal ASARTDL tag, when appended to unrelated reporter proteins, is sufficient to confer secretion in response to ER calcium depletion but not all types of ER stress. This is in agreement with regulation of the MANF protein, which is the origin of the SERCaMP modification. Glembotski *et al.* (2012) showed that tunicamycin, DTT, and thapsigargin all trigger ER stress; however, only thapsigargin induces the secretion of MANF. Other reports indicate that the effects of

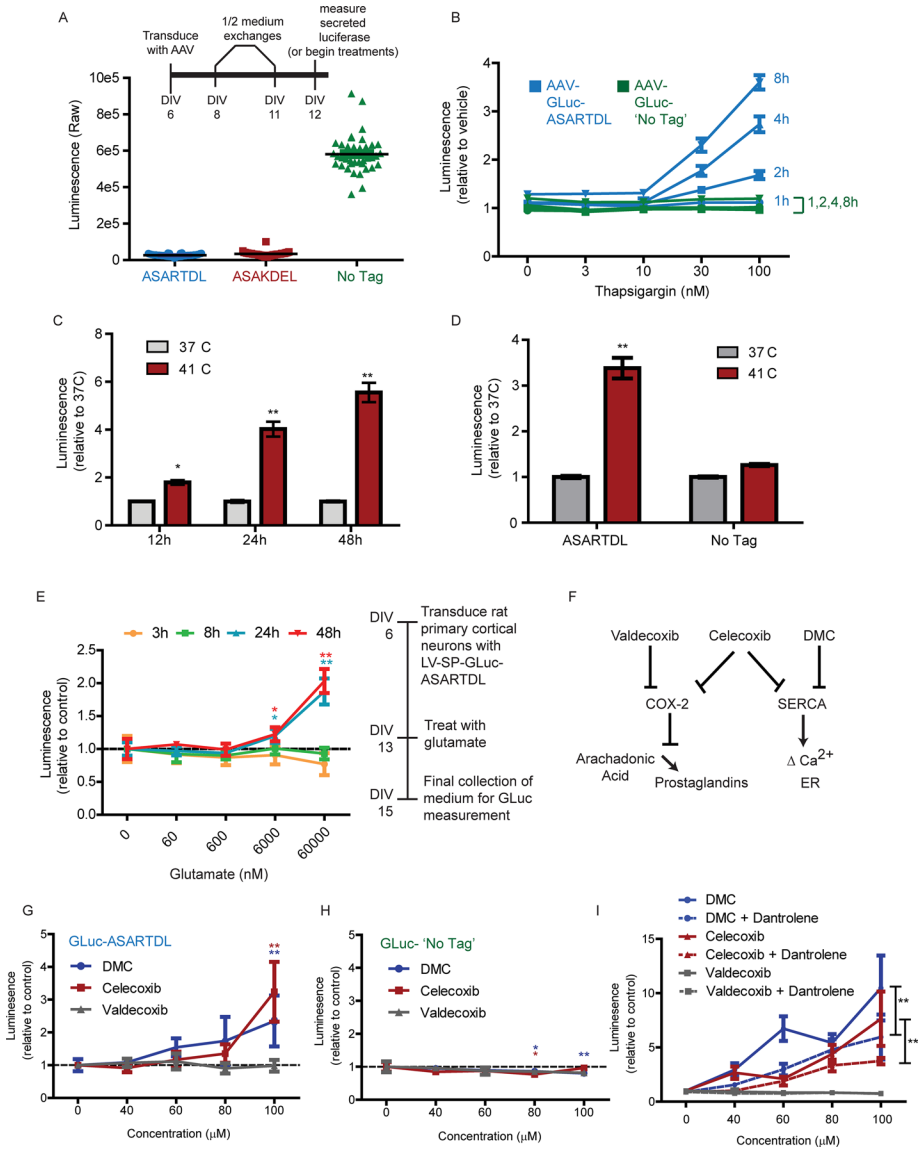


FIGURE 5: Using the GLuc-based SERCaMP to gain insight into calcium dysregulation in primary neurons. (A) Rat PCNs were transduced with AAV-GLuc variants using the time line depicted in the inset, and luciferase was measured in the medium at day in vitro (DIV) 12 ($n = 40$ wells). (B) Rat PCNs were treated on DIV12 with thapsigargin, and secreted luciferase was measured at 1, 2, 4, and 8 h posttreatment (mean ± SEM, $n = 8$). (C) Rat PCNs were transduced with AAV-GLuc-ASARTDL. On DIV13, cells were either shifted to 41°C or maintained at 37°C. *Gaussia* luciferase was measured in the medium at 12, 24, and 48 h (mean ± SEM, $n = 12$, two-way ANOVA; $^*p < 0.05$, $^{**}p < 0.01$ by Bonferroni multiple comparison test). (D) Rat PCNs were equivalently transduced with the ASARTDL or untagged variant of GLuc. Luciferase activity was measured in the medium 48 h after temperature shift (mean ± SEM, $n = 20$, two-way ANOVA; $^{**}p < 0.01$ by Bonferroni multiple comparison test). (E) Rat PCNs were transduced with lentivirus encoding GLuc-ASARTDL. On DIV13, glutamate was added to the cultures, and cells were incubated for 48 h. Luciferase activity was measured in the medium at the indicated time points post glutamate (mean ± SEM, $n = 6$, one-way ANOVA; $^*p < 0.05$; $^{**}p < 0.01$ by Dunnett's multiple comparison test vs. vehicle control). (F) Schematic showing the effect of coxib-type compounds on COX-2 and SERCA. (G, H) Rat PCNs transduced with AAV-GLuc-ASARTDL (G) or untagged AAV-GLuc (H) were treated with valdecoxib, celecoxib, or 2,5- dimethyl-celecoxib on DIV14. Medium was measured for luciferase after 4 h (mean ± SEM, $n = 4$, one-way ANOVA; $^*p < 0.05$; $^{**}p < 0.01$ by Dunnett's multiple comparison test vs. vehicle control). (I) Rat PCNs transduced with AAV-GLuc-ASARTDL or untagged AAV-GLuc were pretreated on DIV13 with 60 μM dantrolene for 30 min before adding the coxibs. Luciferase was measured in the medium after 1.5 h of coxib treatment (mean ± SEM, $n = 4$, two-way ANOVA; $^{**}p < 0.01$ for dantrolene factor).

tunicamycin and DTT on ER calcium are cell-type dependent (Caspersen *et al.*, 2000; Hammadi *et al.*, 2013), and our results suggest that these compounds do not significantly deplete the ER calcium store in SH-SY5Y cells. We anticipate that SERCaMPs will be a useful tool for further delineating the relationship between ER calcium depletion and ER stress in various models.

The Golgi also contains a high concentration of calcium relative to the cytosol, which is in part maintained by the same pumps and channels found in the ER (Pizzo *et al.*, 2011). This overlap makes it challenging to deplete $Ca^{2+}$ pharmacologically from the ER exclusively. Based on our results, it remains possible that depletion of calcium from other compartments of the secretory pathway contributes to the release of SERCaMPs. We attempted to examine the contribution of Golgi calcium using bisphenol, an inhibitor of SPCA, the $Ca^{2+}$ ATPase localized to the *trans*-Golgi (Supplemental Figure S3H; Lai and Michelangeli, 2012). We detected no change in secretion of GLuc-ASARTDL, indicating that any Golgi-based release mechanism would likely be restricted to the early Golgi, where SERCA is localized (Pizzo *et al.*, 2011).

The mechanism that regulates SERCaMP release when ER calcium is depleted remains unknown; however, we found that KDEL receptors are capable of modulating release, similar to our previous observations for MANF (Henderson *et al.*, 2013). We speculate that the KDELR-mediated Golgi-to-ER retrieval process is altered when secretory pathway calcium is depleted. Of note, release of ER luminal proteins containing the canonical KDEL sequence has previously been observed in response to ER calcium imbalance, although the mechanism is unclear (Booth and Koch, 1989). We similarly observed release of KDEL-tagged luciferase (Figures 1, E and J, and 3F), although at a much lower magnitude than for ASARTDL, suggesting the ASARTDL sequence has lower affinity for the KDELR and is more likely to be released after $Ca^{2+}$ depletion. This is consistent with a study that demonstrated that KDELRs more efficiently retain proteins containing a KDEL versus an RTDL tail (Raykhel *et al.*, 2007). Using modified ELISA, we detected an interaction of KDEL receptors with GLuc-SERCaMPs (GLuc-ASARTDL and GLuc-ASAKDEL (Figure 4D); however, the nature of this interaction and its dependence on calcium remain to be determined. Overall we predict that many KDEL-like proteins can be secreted (to different extents) in response to calcium

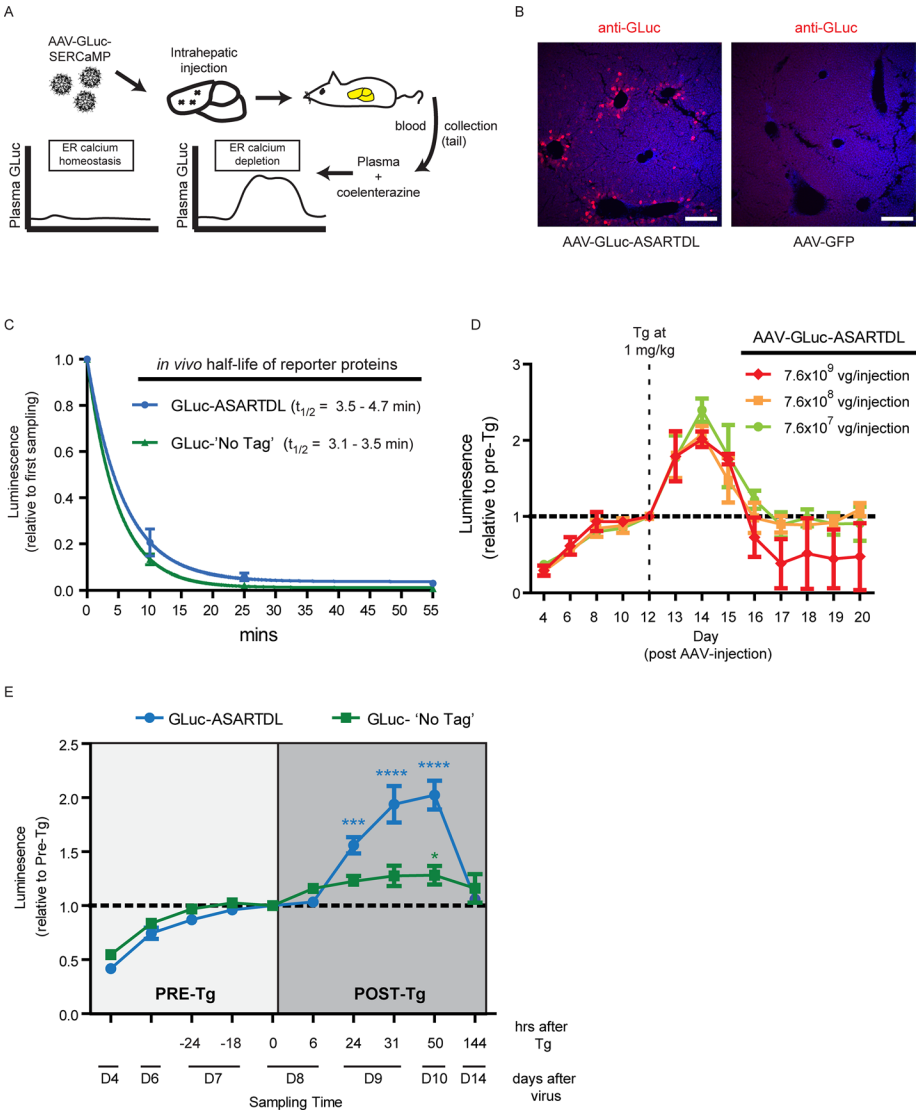


FIGURE 6: AAV-GLuc-ASARTDL is responsive to thapsigargin in an in vivo model. (A) Schema of the in vivo SERCaMP assay. Rats were intrahepatically injected with AAV-GLuc, blood was collected from tail, and plasma was assayed for GLuc activity. (B) Transgene expression in liver was examined by immunohistochemistry. Rats were intrahepatically injected with GLuc-ASARTDL or AAV-GFP and stained with anti-GLuc (red) to examine expression. The viral titer injected ($3 \times 10^{11}$ vg) was ~400-fold higher than in E ($7.6 \times 10^{8}$ vg) to allow for detection by immunohistochemistry. Nuclei were stained with DAPI (blue). Scale bar, 200 µm. (C) Half-life of GLuc proteins in vivo. Conditioned medium collected from stable SH-SY5Y cells was normalized for enzymatic activity and injected into WT rats fitted with a back port connected to the jugular vein, and blood was collected at indicated time points. Half-life is estimated to be <5 min (one-phase decay; 95% confidence interval, 3.5–4.7 min [ASARTDL] and 3.1–3.5 min [No Tag]). Rate of turnover for ASARTDL vs. No Tag was not significantly different (*t* test, $p = 0.92$). (D) Effect of viral titer on SERCaMP release into plasma. Rats received intrahepatic injection of AAV-GLuc-ASARTDL at varying titers ($n = 3$ each). Tg was administered intraperitoneally at 1 mg/kg (on day 12, after sampling blood for "pre" measurement), and luciferase activity was measured in the plasma at the indicated time points (mean ± SEM, normalized to the pre-Tg on day 12). The three viral concentrations displayed similar Tg-induced secretion (two-way ANOVA day12-day15; virus concentration $F(2,21) = 0.48$ [$p = 0.63$]; time factor $F(3,21) = 13.8$ [$p < 0.0001$]). (E) Effect of thapsigargin on plasma levels of GLuc-ASARTDL and GLuc-No Tag was assessed (mean ± SEM, $n = 15$ [ASARTDL], $n = 10$ [No Tag]). The light gray shaded box indicates pre-thapsigargin samples, to monitor the effect of gas isoflurane anesthesia. Blood was collected 6, 24, 31, 50, and 144 h after 1 mg/kg Tg administration, indicated by the dark gray shaded box (ASARTDL: one-way ANOVA, $p < 0.001$; ***$p < 0.001$, ****$p < 0.0001$ by Dunnett's multiple comparison test vs. 0 h; No Tag: 1-way ANOVA, $p = 0.09$; *$p < 0.05$ by Dunnett's multiple comparison test vs. 0 h). Thapsigargin-induced response was greater for ASARTDL than with No Tag (two-way ANOVA, $p < 0.0001$).

depletion and these C-terminal sequences (Raykhel *et al.*, 2007) are good candidates for creating additional SERCaMPs.

The stability of GLuc-SERCaMP in vitro (>72 h in culture medium; Supplemental Figure S1G) and in vivo (<5 min in rat circulation; Figure 6C) was starkly different, which is of importance when interpreting results and designing experiments. In the case of in vitro experiments, in which accumulation is expected to occur, a small volume of medium can be repeatedly sampled from an individual dish or well to track timing of release. Alternatively, washout or perfusion methods can be used to reduce the accumulated background signal. In vivo, the short half-life of GLuc-ASARTDL (<5 min) is a strength, which makes it possible to define more precisely the timing of SERCaMP release. Owing to the rapid turnover, changes in circulating GLuc are indicative of secretion that occurred proximal to sampling and do not represent an accumulation occurring over hours or days. For the case of thapsigargin, we observed elevated GLuc-ASARTDL in plasma after 48 h, suggesting that calcium imbalance in the liver was unresolved after 2 d. We speculate that this protracted GLuc-SERCaMP secretion is due to irreversible SERCA inhibition and persistent calcium depletion in hepatocytes; however, the pharmacokinetics of thapsigargin after systemic exposure and the turnover of SERCA in rat hepatocytes are unknown.

Our in vitro studies using rat primary neurons demonstrate the usefulness of SERCaMPs for monitoring alterations in ER calcium. The models were chosen based on their connection to ER stress, with the goal of determining a temporal relationship between insult and ER calcium homeostasis. In the case of hyperthermia, a report demonstrated that elevated temperature caused decreased SERCA expression in rat PC12 cells (Caspersen *et al.*, 2000). We observed an increased release of GLuc-ASARTDL from rat primary neurons grown at elevated temperature, implicating effects on ER calcium. Glutamate signaling has acute effects on ER calcium through activation of IP3R (Pin and Duvoisin, 1995); however, we did not detect a rapid release of the reporter (Figure 5E). This is consistent with the minimal contribution of IP3Rs observed in other experiments. Alternatively, we observed a delayed release of GLuc-ASARTDL from cells exposed to glutamate. We speculate that the delayed ER calcium imbalance may be due to alterations ER calcium pump function caused by glutamate-induced energy failure (Budd and Nicholls, 1996; Smith *et al.*, 2013).

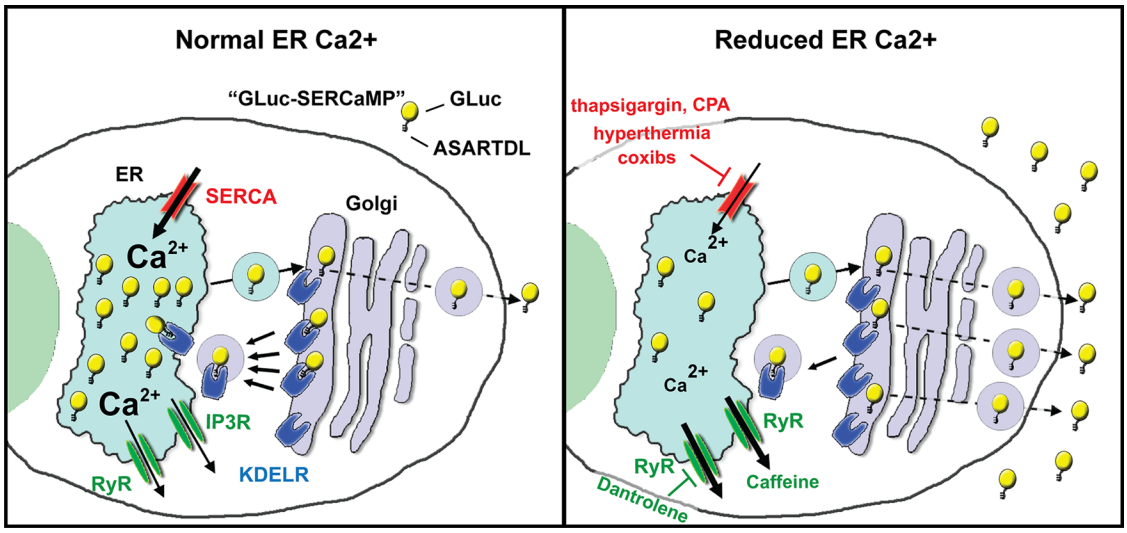


FIGURE 7: Schematic summarizing release of GLuc-SERCaMP in response to ER calcium depletion.

SERCaMPs have potential use in preclinical toxicology studies, which is highlighted by our studies of the coxibs. Although it is now clear that some "selective" coxibs can have off-target effects on SERCA, these compounds were initially considered specific based on an ability to inhibit COX-2 but not COX-1 (Warner *et al.*, 1999). As predicted, the SERCaMP clearly identified the compounds that have known SERCA activities (Figure 5G). We can envision future use of SERCaMPs to screen therapeutics for possible side effects on ER calcium homeostasis, which may signal a potential for toxicity. Of note, the identification of compounds that induce ER calcium depletion may also be a desirable under certain scenarios. For example, coxibs that disrupt SERCA activity are now being considered as potential antitumor agents (Pyrko *et al.*, 2007; Schönthal, 2007). In addition to identifying calcium-disrupting effects, SERCaMPs could also be used to screen for compounds that augment ER calcium homeostasis, which would be of interest in numerous pathological conditions. The low background, high sensitivity, rapid activation, and ability to perform washouts make GLuc-based SERCaMPs amenable to high-throughput approaches.

Whereas current in vivo techniques to monitor ER homeostasis are limited to single time point analyses, we have developed a simple approach that allows for longitudinal assessment of ER calcium homeostasis with repeated sampling of extracellular fluids. Collectively our results indicate that SERCaMPs can be used to monitor ER calcium homeostasis as a component of "ER stress" and will allow a more specific understanding of the underlying mechanisms that govern ER stress pathways. Use of this tool will enhance our ability to characterize progressive diseases associated with ER dysfunction, such as Parkinson's disease and diabetes, for which the cause–effect relationships with ER calcium homeostasis are not fully understood. Moreover, in diseases for which evidence of SERCaMP release is identified, it is plausible that the release of potentially therapeutic trophic factors or hormones can be regulated by the extent of ER calcium dysregulation via SERCaMP modification. This would provide a novel regulatory release mechanism of gene-based therapeutics.

## MATERIALS AND METHODS

### Plasmid construction

Lentiviral GFP plasmids were created through pDONR221 (Life Technologies, Grand Island, NY) intermediates. The pDONR221-SP-GFP entry vector containing the MANF signal peptide was produced by replacing the *Eag*I-*Rsr*II fragment of pDONR221-MANF (Henderson *et al.*, 2013) with the coding region and endogenous stop codon of enhanced GFP. The pDONR221-SP-GFP-RTDL and pDONR221-SP-GFP-KDEL entry vectors were produced by amplifying the SP-GFP open reading frame (from pLenti6.3-SP-GFP) using attB-linked oligos, with the reverse oligo including the nucleotides encoding the ASARTDL or ASAKDEL sequences (Henderson *et al.*, 2013). The lentiviral and AAV vectors encoding *Gaussia* luciferase were created by amplifying the GLuc open reading frame (ORF) from pGLuc-Basic (New England Biolabs, Ipswich, MA) and cloning into the *Eag*I and *Rsr*II sites of a pDONR221-hMANF plasmid. The coding region for GLUC (omitting the signal peptide) was amplified by PCR and recombined into the *Eag*I and *Rsr*II sites using the In-Fusion HD Cloning Kit (Clontech, Mountain View, CA). This effectively replaced hMANF (amino acids [aa] 23–173) with GLUC (aa 19–185), retaining the signal peptide and carboxy-terminal ASARTDL sequences of MANF. For lentivirus, GLuc-ASARTDL was recombined into pLenti6.3 using LR Clonase II (Life Technologies) according to the manufacturer's instructions. The additional carboxy-terminal variants were cloned using attB-linked oligos (reverse oligos to include tail-specific sequences) and pLenti6.3-GLuc-ASARTDL as the template. PCR fragments were inserted into pDONR221 using a BP reaction and moved to pLenti6.3-DEST using an LR reaction. For AAV, the coding region for MANFsp-GLUC-ASARTDL was amplified by PCR and recombined into pdsAAV CMV eGFP, a self-complementary AAV packaging vector (Wang *et al.*, 2003), after removal of the existing eGFP ORF by digestion with *Bam*HI and *Not*I. The amplified inserts and the cloning junctions were verified by sequencing for each vector. All plasmids were propagated in StBl3 recombination-deficient cells (Life Technologies) cultured at 30°C. The myc-FLAG(DDK)–tagged human KDELR ORFs were purchased from Origene, Rockville, MD (KDELR/accession numbers KDELR1/NM_006801.2, KDELR2/NM_006854.2). Lentiviral KDELR plasmids were created by amplifying the ORFs and cloning into the *Bam*HI and *Mlu*I sites of pLenti6.3 using the In Fusion PCR Cloning Kit.

### Lentiviral production and stable cell line generation

The pLenti6.3 expression vectors were packaged into virions using the ViraPower Packaging Mixture (Life Technologies), and lentiviral particles were concentrated by ultracentrifugation on a sucrose

cushion (Han *et al.*, 2009). Lentivirus resuspended in 1× Hank's buffered saline solution was titered using the Lenti-X p24 rapid titer kit (Clontech) and used at a range of MOIs to transduce SH-SY5Y cells plated in 12-well plates. Selection of stable integrants was performed with 2 µg/ml blasticidin over the course of several weeks, until a majority of the cells died. The mixed populations derived from the lentiviral dose that resulted in 3–10 colonies of cells/well were expanded as individual "mixed populations" for further experimentation.

### AAV packaging and purification

All vectors were prepared by a triple transfection method as previously described in HEK293 cells (Howard *et al.*, 2008). Cell and media pellets were thawed and combined, then freeze-thawed two times, vortexing after each thaw. $MgCl_2$ (2 mM final; Sigma-Aldrich, St. Louis, MO) and Benzonase (EMD Millipore, Billerica, MA) were added at 50 U/ml of cell solution for 1 h at 37°C with continuous shaking. The solution was centrifuged for 20 min at 2450 × *g* at 4°C. The supernatant was transferred to 75 ml of phosphate-buffered saline (PBS) with 2 mM $MgCl_2$ and sequentially filtered through 5-, 0.45-, and 0.22-µm filters. The solution was then run through a 1 ml of AVB Sepharose HI-TRAP column (GE Healthcare, Pittsburgh, PA) using an AKTA purifier (GE Healthcare) at a rate of 2 ml/min and eluted using a 15 mM sodium citrate solution (Sigma-Aldrich) at a rate of 1 ml/min. The fractions containing the peak of the $OD_{254}$ and $OD_{280}$ readings were collected and dialyzed using a 10,000 MWCO dialysis cassette (Pierce, now Thermo Fisher Scientific, Rockford, IL) in 1 l of PBS containing 0.5 mM $MgCl_2$ for three exchanges over 25–30 h. The equilibrated virus was aliquoted, snap-frozen, and stored at –70°C.

### AAV titering

Titers were calculated as viral genomes based on a standard curve using a pdsAAV-CMV-MANFsigpep-GLUC-KAASARTDL plasmid linearized with EcoRI (New England Biolabs). The linearized plasmid was diluted in PBS to $1 \times 10^{-1}$ to $10^{-5}$ ng/ml. A viral aliquot was thawed, sonicated for 10 s in a Fisher 180z ultrasonic cleaner (Fisher Scientific), and serially diluted from 1:1000 to 1:10,000 in PBS (Life Technologies). Standards and viruses (triplicates) were assayed by TaqMan Universal PCR Master Mix (Life Technologies) with the following reaction conditions: 95°C × 5 min, 94°C × 20 s, and 60°C × 1 min for 41 cycles. The following GLuc primers and probe (Integrated DNA Technologies, San Jose, CA) were used: forward, 5′-CACGCCCAAGATGAAGAAGT-3′; reverse, 5′-GAACCCAGGAATCTCAGGAATG-3′; probe (5′-6-FAM/3′-BHQ-1 labeled), 5′-TACGAAGGCGACAAAGAGTCCGC-3′. Real-time PCRs were run on a CFX96 (Bio-Rad, Hercules, CA). The standard curve was used to calculate viral genomes/milliliter of the AAV.

### Cell culture

SH-SY5Y neuroblastoma cells were maintained as previously described (Henderson *et al.*, 2013). Rat primary cortical cultures were prepared as described previously (Howard *et al.*, 2008) and in accordance with approved procedures by the National Institutes of Health Animal Care and Usage Committee. We plated $6.0 \times 10^4$ cells in polyethyleneimine-coated wells (96-well plate) and performed half-medium exchanges on days 4, 6, 8, 11, and 13. Viral transductions were performed on day 6 in culture. For hyperthermia experiments, cells were cultured at elevated temperature (41°C) as described. Temperatures were monitored every 30 s using a temperature data logger equipped with a K-type thermocouple probe (Omega, Stamford, CT).

### Antibodies and other reagents

The antibodies used were monoclonal GFP (Roche Applied Science, Indianapolis, IN), monoclonal actin (clone C4; Abcam, Cambridge, MA), polyclonal actin (Sigma-Aldrich), polyclonal *Gaussia* luciferase (New England Biolabs), polyclonal BiP (Cell Signaling, Danvers, MA), monoclonal FLAG (clone M2; Sigma-Aldrich), and monoclonal Myc (clone 4A6; Millipore). Chemicals used (with diluent in parentheses) were thapsigargin (dimethyl sulfoxide [DMSO] in in vitro studies, ethanol in in vivo studies; Sigma-Aldrich), cycloheximide (DMSO; Sigma-Aldrich), brefeldin A (ethanol; Sigma-Aldrich), dithiothreitol (water; Sigma-Aldrich), tunicamycin (DMSO; Sigma-Aldrich), cyclopiazonic acid (DMSO; Sigma-Aldrich), A23187 (DMSO; Sigma-Aldrich), TPEN (DMSO; Sigma-Aldrich), dantrolene (DMSO; Sigma-Aldrich), xestospongin C (DMSO; Sigma-Aldrich), caffeine (water; Sigma-Aldrich), glutamate (1 N HCl; Sigma-Aldrich), celecoxib (DMSO; Sigma-Aldrich), valdecoxib (DMSO; Sigma-Aldrich), and 2,5-dimethyl-celecoxib (DMSO; Sigma-Aldrich). Vehicle controls at concentrations equivalent to treatments were used in all experiments. Cell viability assays were performed with the CellTiter 96 $AQ_{ueous}$ One Solution Cell Proliferation Assay (MTS) or the CellTiter-Glo Luminescent Cell Viability Assay (ATP) following the manufacturer's instructions (Promega, Madison, WI).

### *Gaussia* luciferase secretion assay

For luciferase secretion assays, 5 µl of culture medium was removed from a well and transferred to an opaque-walled plate (multiple time points collected from the same 96-well plate of cells). GLuc substrate was PBS containing an additional 5 mM NaCl and 10 µM coelenterazine (Regis Technologies, Morton Grove, IL). Coelenterazine stock solutions were prepared at 20 mM in acidified methanol (10 µl of 10 N HCl/1 ml of methanol) and stored at –80°C as single-use aliquots. Prepared substrate was incubated at room temperature for 30 m before use. Amount of luciferase was determined using a plate reader with an injector setup (Biotek Synergy II, Winooski, VT) to allow for immediate read of sample after injection. Typically, 100 µl of substrate was injected to the well containing cell culture medium. For secretion assays, vehicle controls were used in all experiments at concentration equivalent to the treatments. For the TPEN assays, extracellular calcium was chelated by exchanging medium with fresh SH-SY5Y medium containing 1.8 mM ethylene glycol tetraacetic acid before the addition of TPEN.

### GFP-based secretion assay

Methods are described in detail in Henderson *et al.* (2013). In brief, medium was collected and measured for GFP fluorescence on a Biotek SynergyII using excitation at 485/20 and emission at 528/20 filters (BioTek).

### Immunocytochemistry and immunohistochemistry

Cells were seeded in six-well plates on 25-mm round glass coverslips (Warner Instruments, Hamden, CT) at $4.0 \times 10^5$ cells and allowed to grow overnight. Cells were transfected with DsRed-ER (Clontech) using 0.4 µg of DNA and 2 µl of Lipofectamine 2000 (Life Technologies) per well. After 24 h, cells were fixed in 4% paraformaldehyde (in 1× PBS, pH 7.4), permeabilized with PBS/0.1% Triton-X, blocked for 1 h with PBS/0.1% Triton X/2% bovine serum albumin (BSA)/5% goat serum, and immunostained with anti–*Gaussia* luciferase. Cells were mounted on glass sides with Mowiol 4-88 (EMD) and imaged using a confocal microscope (Nikon Eclipse C1; Melville, NY) equipped with a 60× objective (1.4 numerical aperture [NA]). Images were acquired with Nikon EZ C1 software and processed in Adobe Photoshop (San Jose, CA). For rat liver immunohistochemistry,

100 µl of virus diluted to $3.1 \times 10^{12}$ vg/ml in saline was injected into the liver at three different locations with a 30-gauge needle. AAV-eGFP was used as a control. At 18 d postinjection, animals were perfused with 4% paraformaldehyde, and livers were excised and transferred to 18% sucrose. Frozen livers were sectioned on a Leica cryostat (40 µm; Leica Microsystems; Buffalo Grove, IL), stained with anti-GLuc (New England Biolabs) and anti-GFP (Roche), both at 1:500, and mounted to glass slides. Images were captured with using a Nikon Eclipse E800 equipped with QImaging Rolera em-$c^2$ camera and a 10× objective (0.45 NA).

### Western blot

Cells were lysed in a modified RIPA buffer containing 50 mM Tris-HCl (pH 7.4), 0.25% sodium deoxycholate, 150 mM NaCl, 1 mM EDTA, 1% Nonidet P-40, and 1× protease inhibitor mixture. After quantifying samples using a DC assay (Bio-Rad), equal amounts of total protein were separated on 4–12% NuPAGE gels using 3-(*N*-morpholino)propanesulfonic acid or 2-(*N*-morpholino)ethanesulfonic acid (MES) running buffer. Proteins were transferred to 0.20-µm polyvinylidene fluoride membranes (Life Technologies) and immunoblotted with the primary antibodies described earlier and LI-COR blocking reagent (LI-COR Biosciences, Lincoln, NE). Secondary antibodies were IR700 and IR800 (Rockland Immunochemicals, Gilbertsville, PA), and blots were scanned using an Odyssey scanner (LI-COR).

### KDELR microplate interaction assay

Maxisorp 96-well plates (Nunc, now Thermo Fisher Scientific, Rockford, IL) were coated with 1 µg of antibody (or immunoglobulin control, or no antibody control) per well diluted in 50 mM bicarbonate/carbonate binding buffer (pH 9.6). Antibodies were allowed to adhere overnight and washed twice in 200 µl of PBS. Wells were blocked with PBS/2% BSA for 3 h at room temperature. Protein lysates were collected from SH-SY5Y cells transfected for 48 h with pCMV6-KDELR1-myc-DDK using a buffer containing 25 mM MES hydrate (pH 6.4 at 4°C), 110 mM NaCl, 1 mM $CaCl_2$, 1% 3-[(3-cholamidopropyl)dimethylammonio]-1-propanesulfonate (CHAPS), and protease inhibitors. Lysates containing myc-FLAG–tagged KDELR1 were diluted 1:10 in the foregoing buffer without detergent (final CHAPS, 0.1%), added to the wells, and incubated overnight at 4°C. After binding, wells were washed four times with the 25 mM MES hydrate (pH 6.4 at 4°C), 110 mM NaCl, 1 mM $CaCl_2$, 0.1% CHAPS, and protease inhibitors. Supernatants collected from stable SH-SY5Y cells expressing the GLuc variants were normalized to equivalent luciferase RLUs using conditioned medium from parental SH-SY5Y cells. Supernatants were spun at 2000 × *g* for 5 min to pellet large debris and dialyzed using Slide-A-Lyzer dialysis cassettes (Pierce) into 25 mM MES hydrate (pH 6.4 at 4°C), 110 mM NaCl, and 1 mM $CaCl_2$. Three exchanges of 1.5 l of dialysis buffer were performed over 24 h at 4°C. CHAPS was added to the dialyzed supernatants to a final concentration of 0.1%, and then samples were added to the KDELR1-coated microplate and incubated overnight at 4°C. Wells were washed on ice four times with 200 µl of 25 mM MES hydrate (pH 6.4 at 4°C), 110 mM NaCl, 1 mM $CaCl_2$, 0.1% CHAPS, and protease inhibitors. After the final wash, 100 µl of PBS was added to each well and incubated at room temperature for 20 min before injection of coelenterazine substrate as described for the GLuc secretion assays.

### In vivo *Gaussia* luciferase assays

All animal procedures were performed in accordance with National Institutes of Health Animal Care Guidelines. Male Sprague Dawley rats received intrahepatic injections of AAV-GLuc-ASARTDL or AAV-GLuc under anesthesia. Virus (100 µl diluted to $7.6 \times 10^9$ vg/ml) was injected into the liver at three different locations (~33 µl per site) with a 30-gauge needle. For blood collection, animals were anesthetized with gas anesthesia, tails clipped, and blood collected into tubes prefilled with heparin (50 µl at 1000 U/ml). The ratio of blood to heparin was normalized for all samples to 2:1 before further processing. Samples were centrifuged at 2000 × *g* for 5 min at 4°C to isolate plasma, which was stored at –80°C until time of luciferase assay. Animals received a single i.p. injection of thapsigargin (Sigma-Aldrich; 1 mg/kg) on day 8. For luciferase assays, 10 µl of plasma was transferred to an opaque walled plate and substrate PBS + 100 µM coelenterazine + 500 mM ascorbic acid to reduce substrate oxidation) was injected using an automated plate reader as described above.

### *Gaussia* luciferase half-life

Male Sprague Dawley rats underwent jugular catheterization under anesthesia. Catheters were connected to a back port (Plastics One, Roanoke, VA); catheter patency was assessed with heparinized saline following port implantation and sealed with port cap to prevent coagulation. Three days post–catheter implantation, GLuc-ASARTDL half-life was measured in animals without anesthesia. Briefly, 400 µl of conditioned medium from SH-SY5Y-GLuc-ASARTDL cells was infused through back ports. Ports were immediately flushed with heparinized saline following media infusion. Blood was collected 5, 15, 30, and 60 min following media infusion into tubes prefilled with heparin (50 µl at 1000 U/ml). The ratio of blood to heparin was normalized for all samples to 2:1 before further processing. From this point forward, samples were handled as those described above. Half-life was calculated using a one-phase decay model (GraphPad Prism6; La Jolla, CA).

## ACKNOWLEDGMENTS

We thank Doug Howard, Lowella Fortuno, Josh Hinkle, Ray Rogers, Rodden Reyes, and Jennifer Bossert for technical assistance. We also thank Tsung-Ping Su, Bruce Hope, Marc Halterman, Mart Saarma, and Mikko Airavaara for critical reading of the manuscript and Deon Harvey for assistance with figure preparation. This work was supported by the Intramural Research Program, National Institute on Drug Abuse.

## REFERENCES

Badr CE, Hewett JW, Breakefield XO, Tannous BA (2007). A highly sensitive assay for monitoring the secretory pathway and ER stress. PLoS One 2, e571.

Booth C, Koch GL (1989). Perturbation of cellular calcium induces secretion of luminal ER proteins. Cell 59, 729–737.

Budd SL, Nicholls DG (1996). Mitochondria, calcium regulation, and acute glutamate excitotoxicity in cultured cerebellar granule cells. J Neurochem 67, 2282–2291.

Burdakov D, Petersen OH, Verkhratsky A (2005). Intraluminal calcium as a primary regulator of endoplasmic reticulum function. Cell Calcium 38, 303–310.

Caspersen C, Pedersen PS, Treiman M (2000). The sarco/endoplasmic reticulum calcium-ATPase 2b is an endoplasmic reticulum stress-inducible protein. J Biol Chem 275, 22363–22372.

Davidson GA, Varhol RJ (1995). Kinetics of thapsigargin-Ca(2+)-ATPase (sarcoplasmic reticulum) interaction reveals a two-step binding mechanism and picomolar inhibition. J Biol Chem 270, 11731–11734.

Di Jeso B, Pereira R, Consiglio E, Formisano S, Satrustegui J, Sandoval IV (1998). Demonstration of a Ca2 +requirement for thyroglobulin dimerization and export to the Golgi complex. Eur J Biochem 252, 583–590.

Fu S, Yang L, Li P, Hofmann O, Dicker L, Hide W, Lin X, Watkins SM, Ivanov AR, Hotamisligil GS (2011). Aberrant lipid metabolism disrupts calcium

homeostasis causing liver endoplasmic reticulum stress in obesity. Nature 473, 528–531.
Gillard EF, Otsu K, Fujii J, Duff C, de Leon S, Khanna VK, Britt BA, Worton RG, MacLennan DH (1992). Polymorphisms and deduced amino acid substitutions in the coding sequence of the ryanodine receptor (RYR1) gene in individuals with malignant hyperthermia. Genomics 13, 1247–1254.
Glembotski CC, Thuerauf DJ, Huang C, Vekich JA, Gottlieb RA, Doroudgar S (2012). Mesencephalic astrocyte-derived neurotrophic factor (MANF) protects the heart from ischemic damage and is selectively secreted upon ER calcium depletion. J Biol Chem 287, 25893–25904 .
Hammadi M, Oulidi A, Gackière F, Katsogiannou M, Slomianny C, Roudbaraki M, Dewailly E, Delcourt P, Lepage G, Lotteau S, *et al.* (2013). Modulation of ER stress and apoptosis by endoplasmic reticulum calcium leak via translocon during unfolded protein response: involvement of GRP78. FASEB J 27, 1600–1609.
Han X, Qian X, Bernstein JG, Zhou HH, Franzesi GT, Stern P, Bronson RT, Graybiel AM, Desimone R, Boyden ES (2009). Millisecond-timescale optical control of neural dynamics in the nonhuman primate brain. Neuron 62, 191–198.
Hara M, Bindokas V, Lopez JP, Kaihara K, Landa LR, Harbeck M, Roe MW (2004). Imaging endoplasmic reticulum calcium with a fluorescent biosensor in transgenic mice. Am J Physiol Cell Physiol 287, C932–938.
Henderson MJ, Richie CT, Airavaara M, Wang Y, Harvey BK (2013). Mesencephalic astrocyte-derived neurotrophic factor (MANF) secretion and cell surface binding are modulated by KDEL receptors. J Biol Chem 288, 4209–4225.
Herrmann-Frank A, Richter M, Sarközi S, Mohr U, Lehmann-Horn F (1996). 4-Chloro-m-cresol, a potent and specific activator of the skeletal muscle ryanodine receptor. Biochim Biophys Acta 1289, 31–40.
Hofer AM, Fasolato C, Pozzan T (1998). Capacitative Ca2+ entry is closely linked to the filling state of internal Ca2+ stores: a study using simultaneous measurements of ICRAC and intraluminal [Ca2+]. J Cell Biol 140, 325–334.
Howard DB, Powers K, Wang Y, Harvey BK (2008). Tropism and toxicity of adeno-associated viral vector serotypes 1, 2, 5, 6, 7, 8, and 9 in rat neurons and glia in vitro. Virology 372, 24–34.
Johnson AJ, Hsu AL, Lin HP, Song X, Chen CS (2002). The cyclo-oxygenase-2 inhibitor celecoxib perturbs intracellular calcium by inhibiting endoplasmic reticulum Ca2+-ATPases: a plausible link with its anti-tumour effect and cardiovascular risks. Biochem J 366, 831–837.
Lai P, Michelangeli F (2012). Bis(2-hydroxy-3-tert-butyl-5-methyl-phenyl)-methane (bis-phenol) is a potent and selective inhibitor of the secretory pathway $Ca^{2+}$ ATPase (SPCA1). Biochem Biophys Res Commun 424, 616–619.
Lanner JT, Georgiou DK, Joshi AD, Hamilton SL (2010). Ryanodine receptors: structure, expression, molecular details, and function in calcium release. Cold Spring Harb Perspect Biol 2, a003996.
Lee AS (2005). The ER chaperone and signaling regulator GRP78/BiP as a monitor of endoplasmic reticulum stress. Methods 35, 373–381.
Lindholm P, Voutilainen MH, Lauren J, Peränen J, Leppänen VM, Andressoo JO, Lindahl M, Janhunen S, Kalkkinen N, Timmusk T, *et al.* (2007). Novel neurotrophic factor CDNF protects and rescues midbrain dopamine neurons in vivo. Nature 448, 73–77.
Mattson MP, LaFerla FM, Chan SL, Leissring MA, Shepel PN, Geiger JD (2000). Calcium signaling in the ER: its role in neuronal plasticity and neurodegenerative disorders. Trends Neurosci 23, 222–229.
Mekahli D, Bultynck G, Parys JB, De Smedt H, Missiaen L (2011). Endoplasmic-reticulum calcium depletion and disease. Cold Spring Harb Perspect Biol 3, pii: a004317.
Micaroni M (2010). The role of calcium in intracellular trafficking. Curr Mol Med 10, 763–773.
Odermatt A, Taschner PE, Khanna VK, Busch HF, Karpati G, Jablecki CK, Breuning MH, MacLennan DH (1996). Mutations in the gene-encoding SERCA1, the fast-twitch skeletal muscle sarcoplasmic reticulum Ca2+ ATPase, are associated with Brody disease. Nat Genet 14, 191–194.
Palmer AE, Jin C, Reed JC, Tsien RY (2004). Bcl-2-mediated alterations in endoplasmic reticulum Ca2 +analyzed with an improved genetically encoded fluorescent sensor. Proc Natl Acad Sci USA 101, 17404–17409.
Pin JP, Duvoisin R (1995). The metabotropic glutamate receptors: structure and functions. Neuropharmacology 34, 1–26.
Pizzo P, Lissandron V, Capitanio P, Pozzan T (2011). Ca(2+) signalling in the Golgi apparatus. Cell Calcium 50, 184–192.
Pyrko P, Kardosh A, Liu YT, Soriano N, Xiong W, Chow RH, Uddin J, Petasis NA, Mircheff AK, Farley RA, *et al.* (2007). Calcium-activated endoplasmic reticulum stress as a major component of tumor cell death induced by 2,5-dimethyl-celecoxib, a non-coxib analogue of celecoxib. Mol Cancer Ther 6, 1262–1275.
Raykhel I, Alanen H, Salo K, Jurvansuu J, Nguyen VD, Latva-Ranta M, Ruddock L (2007). A molecular specificity code for the three mammalian KDEL receptors. J Cell Biol 179, 1193–1204.
Rehberg M, Lepier A, Solchenberger B, Osten P, Blum R (2008). A new non-disruptive strategy to target calcium indicator dyes to the endoplasmic reticulum. Cell Calcium 44, 386–399.
Rutkowski DT, Kaufman RJ (2004). A trip to the ER: coping with stress. Trends Cell Biol 14, 20–28.
Sakuntabhai A, Ruiz-Perez V, Carter S, Jacobsen N, Burge S, Monk S, Smith M, Munro CS, O'Donovan M, Craddock N, *et al.* (1999). Mutations in ATP2A2, encoding a Ca2+ pump, cause Darier disease. Nat Genet 21, 271–277.
Schönthal AH (2007). Direct non-cyclooxygenase-2 targets of celecoxib and their potential relevance for cancer therapy. Br J Cancer 97, 1465–1468.
Seidler NW, Jona I, Vegh M, Martonosi A (1989). Cyclopiazonic acid is a specific inhibitor of the Ca2+-ATPase of sarcoplasmic reticulum. J Biol Chem 264, 17816–17823.
Smith IC, Bombardier E, Vigna C, Tupling AR (2013). ATP consumption by sarcoplasmic reticulum $Ca^{2+}$ pumps accounts for 40–50% of resting metabolic rate in mouse fast and slow twitch skeletal muscle. PLoS One 8, e68924.
Sobrevals L, Enguita M, Rodriguez C, Gonzalez-Rojas J, Alzaguren P, Razquin N, Prieto J, Fortes P (2012). AAV vectors transduce hepatocytes in vivo as efficiently in cirrhotic as in healthy rat livers. Gene Ther 19, 411–417.
Sokka AL, Putkonen N, Mudo G, Pryazhnikov E, Reijonen S, Khiroug L, Belluardo N, Lindholm D, Korhonen L (2007). Endoplasmic reticulum stress inhibition protects against excitotoxic neuronal injury in the rat brain. J Neurosci 27, 901–908.
Tang S, Wong HC, Wang ZM, Huang Y, Zou J, Zhuo Y, Pennati A, Gadda G, Delbono O, Yang JJ (2011). Design and application of a class of sensors to monitor Ca2+ dynamics in high Ca2+ concentration cellular compartments. Proc Natl Acad Sci USA 108, 16265–16270.
Taylor CW, Tovey SC (2010). IP(3) receptors: toward understanding their activation. Cold Spring Harb Perspect Biol 2, a004010.
Wang Z, Ma HI, Li J, Sun L, Zhang J, Xiao X (2003). Rapid and highly efficient transduction by double-stranded adeno-associated virus vectors in vitro and in vivo. Gene Ther 10, 2105–2111.
Warner TD, Giuliano F, Vojnovic I, Bukasa A, Mitchell JA, Vane JR (1999). Nonsteroid drug selectivities for cyclo-oxygenase-1 rather than cyclo-oxygenase-2 are associated with human gastrointestinal toxicity: a full in vitro analysis. Proc Natl Acad Sci USA 96, 7563–7568.
Xu X, Gupta S, Hu W, McGrath BC, Cavener DR (2011). Hyperthermia induces the ER stress pathway. PLoS One 6, e23740.